Eur. Phys. J. D **4**, 15–29 (1998)

THE EUROPEAN PHYSICAL JOURNAL D

Adiabatic population transfer in multistate chains via dressed intermediate states

N.V. Vitanov[1,a], B.W. Shore[2,3], and K. Bergmann[3]

[1] Helsinki Institute of Physics, P.O. Box 9, 00014 University of Helsinki, Finland
[2] Lawrence Livermore National Laboratory, Livermore, CA 94550, USA
[3] Fachbereich Physik der Universität, 67653 Kaiserslautern, Germany

Received: 17 April 1998 / Accepted: 15 June 1998

Abstract. The well-known process of stimulated Raman adiabatic passage (STIRAP) provides a robust technique for achieving complete population transfer between the first and last state of a three-state chain, with little population, even transiently, in the intermediate state. The extension of STIRAP to general N-state chainwise-linked systems continues to generate interest. Recently Malinovsky and Tannor (Phys. Rev. A **56**, 4929 (1997)) have shown with numerical simulation that a resonant pulse sequence, which they term "straddle STIRAP", can produce (under appropriate conditions, including specific pulse areas) complete population transfer with very little population in intermediate states. Their proposal supplements a pair of counterintuitively ordered delayed laser pulses, driving the first and last transition of the chain and corresponding to the pump and Stokes pulses in STIRAP, with one or more additional strong pulses of longer duration which couple the intermediate transition(s) and overlap both the pump and the Stokes pulses. In this paper, we modify the "straddling" Malinovsky-Tannor pulse sequence so that the intermediate couplings are *constant* (and strong), at least during the times when the pump and Stokes pulses are present, and the intermediate states therefore act as a strongly coupled subsystem with constant eigenvalues. Under this condition, we show that the original N-state chain is mathematically equivalent to a system comprising $N-2$ parallel Λ-transitions, in which the initial state is coupled simultaneously to $N-2$ dressed intermediate states, which in turn are coupled to the final state. The population transfer is optimized by suitably tuning the pump and Stokes frequencies to resonance with one of these dressed intermediate states, which effectively acts as the single intermediate state in a three-state STIRAP-like process. We show that tuning to a dressed intermediate state turns the system (for both odd N and even N) into a three-state system – with all of the properties of conventional STIRAP (complete population transfer, little transient population in the intermediate states, insensitivity to variations in the laser parameters, such as pulse area). The success of the tuning-to-dressed-state idea is explained by using simple analytic approaches and illustrated with numerical simulations for four-, five-, six- and seven-state systems.

PACS. 32.80.Bx Level crossing and optical pumping – 33.80.Be Level crossing and optical pumping – 42.50.-p Quantum optics

1 Introduction

One of the important uses of laser radiation in atomic and molecular physics derives from the possibility of producing complete transfer of population from an initially populated bound state to a preselected single target state. Over the years, various techniques have been proposed to achieve this objective, including the use of pulses having precise fluences (*i.e.* π-pulses for two-state atoms) and pulses whose carrier frequency sweeps across a Bohr transition frequency (*i.e.* adiabatic passage induced by chirped pulses) [1]. One of the more recent proposals, stimulated Raman adiabatic passage (STIRAP), has become an established technique for efficient population transfer in three-state systems in Λ or ladder configurations. The basic, original STIRAP concept deals with three states, an initial state ψ_1, a final target state ψ_3, and an intermediate state ψ_2, excited by two partially overlapping pulses, a pump pulse linking the initial state with the intermediate state, and a Stokes pulse linking the intermediate state with the final target state. By applying the Stokes pulse before the pump pulse (thereby creating a coherent superposition "trapped" state), and maintaining adiabatic-evolution conditions, one ensures population transfer from the initial state into the final state, with negligible population in the intermediate state at any time. In the ideal limit, unit transfer efficiency is guaranteed and the process is robust against moderate changes in the laser parameters. STIRAP has been studied in detail theoretically

[a] e-mail: vitanov@rock.helsinki.fi

([2–10] and references therein) and realized experimentally [11–19].

The success of STIRAP has encouraged its extensions to multistate systems. In particular, the effects of multiple intermediate and final states, which are usually present in a realistic experimental situation, have been investigated [20–25]. It has been found that the presence of other states near the (resonant) original intermediate state does not markedly influence the transfer efficiency. It has also been shown that, because of the narrow two-photon line width [26–28], STIRAP very selectively targets a particular final state in the presence of linkages to other nearby states.

A considerable literature is now devoted to extending STIRAP to chainwise-linked multistate systems $\psi_1 \leftrightarrow \psi_2 \leftrightarrow \psi_3 \leftrightarrow \ldots \leftrightarrow \psi_N$. Some extensions use only the original two pulses (pump and Stokes) [29–31], whereas other proposals (including the present work) assume additional independent pulses [31–33].

In systems with an *odd* number of states, it has been shown that a similar population transfer process can take place for delayed and counterintuitively ordered pulses in the case when all lasers are on resonance with the corresponding transitions or when only the even states in the chain are detuned from resonance [29–31]. Such a multistate transfer has indeed been achieved experimentally [34–37]. In systems with an *even* number of states, and in particular for four-state systems, it has been concluded that in the on-resonance case, no STIRAP-like process can take place and the transfer efficiency oscillates as the laser intensity increases [31,32]. It has been found that a STIRAP-like transfer can only occur for nonzero intermediate-state detunings [31,32].

A substantial difference between the conventional three-state STIRAP and the multistate extensions is that in the latter at least some intermediate states are populated during the transfer and may acquire significant transient populations, even in the adiabatic regime. Such population is undesirable if these states undergo appreciable spontaneous emission during times of interest. Recently, Malinovsky and Tannor have shown [33], on the basis of numerical results obtained by using a variation of optimal-control theory, that the intermediate populations can be suppressed when the pulses, coupling the intermediate transitions, are much stronger than the pump and Stokes pulses, driving the first and the last transitions. They have suggested a pulse sequence, in which all intermediate pulses arrive simultaneously with the Stokes pulse and vanish simultaneously with the pump pulse, and they have termed it "straddle-STIRAP". Diminution of the intermediate populations by the intermediate couplings has also been noted earlier in the case of constant couplings ([38,39], see also [1]). The success of the Malinovsky-Tannor scheme [33] in dramatically reducing the intermediate-state populations is an important step for practical implementation of multistate population transfer. Our present work extends their study and, most importantly, provides a rationale (*via* dressed states analysis) for the understanding of the success of this aspect of their scheme.

Very recently, the general conditions under which a STIRAP-like population transfer can (or cannot) take place from state ψ_1 to state ψ_N in chainwise-linked N-state systems, and the conditions for minimization of the intermediate populations have been derived analytically for odd and even numbers of states [40]. It has been demonstrated that using a counterintuitive pulse sequence in addition to adiabatic evolution is not sufficient to enable a STIRAP-like population transfer, but there are also certain conditions on the laser parameters (detunings and Rabi frequencies) to be met. It has been shown that the systems with odd and even N behave very differently in the on-resonance case, whereas the off-resonance behavior is rather similar.

We note that, in addition to the excitation schemes based on counterintuitively ordered pulses, numerous authors have examined schemes for achieving complete population transfer in multilevel systems by using frequency-swept pulses [41–44].

In the present paper, we combine various earlier ideas with new ones into a scheme which bears all important features of STIRAP and can be seen as its genuine extension to chainwise-linked multistate systems. The scheme enables an adiabatic-transfer process between the initial and the final states of the chain with unity transfer efficiency and little or no transient populations in the intermediate states. It is based on supplementing a pair of counterintuitively ordered delayed laser pulses, driving the first and last transition of the chain and corresponding to the pump and Stokes pulses in STIRAP, with an additional independent control pulse (or pulses) which couples the intermediate transition(s), as in [31–33]. Following [33], we require that this pulse(s) is strong, in order to suppress the transient populations in the intermediate states. We also require that the control pulses are of longer, overlapping duration, so that they can be considered nearly *constant* during the times when the pump and Stokes pulses are present. A key point in our analysis is the observation that the control pulses couple the $N-2$ intermediate states into a *dressed system*, prior to the arrival of the pump and Stokes pulses. We adopt the term *control* pulses because by changing their parameters (intensities and frequencies) we can effectively establish the properties of this dressed subsystem and hence, control the population transfer process. We show that by suitably tuning the pump and Stokes lasers to one of the dressed eigenvalues of this subsystem, we obtain an effective three-state system of strongly coupled states. Within this three-state approximation we can produce an efficient STIRAP-like population transfer from state ψ_1 to state ψ_N. We will demonstrate that the tuning-to-eigenvalue approach not only complies with the general conditions for STIRAP-like multistate transfer [40], but it *optimizes* the transfer. Our requirement for constant control lasers derives from the fact that then the dressed eigenenergies are constant too and hence, the resonance with the particular dressed state can be maintained throughout the excitation process. Moreover, then the chainwise N-state system is equivalent to a parallel multi-Λ system comprising the first state ψ_1 and the last state ψ_N of the chain, and $N-2$ (dressed) states, each of which is only coupled to states ψ_1 and ψ_N. Thus, we establish a similarity between the chainwise-linked multistate systems and the parallel superposed multi-Λ systems studied in the context of the effect of other states near the intermediate state in the standard STIRAP [20–25], as mentioned above. Finally, we note that the idea of tuning to an eigenvalue of the dressed intermediate subsystem has been mentioned for the first time in [31] in the case of a four-state system. Here we analyse it in detail and extend it to the general case of N-state systems.

Our paper is organized as follows. In Section 2, we present the basic equations and definitions and review the standard three-state STIRAP. In Section 3, we discuss four-state systems, which allow us to demonstrate explicitly our idea of tuning to resonance with a dressed intermediate state. In Section 4, we consider the general case of N-state systems and present numerical results for four- through seven-state systems which follow very accurately our analytical predictions. Finally, in Section 5, we summarize the conclusions.

2 Basic equations and definitions

2.1 Basic STIRAP

The Schrödinger equation for the probability amplitudes $C_k(t)$, associated with atomic states ψ_k $(k=1,2,\ldots,N)$, under the influence of a time varying Hamiltonian $H(t)$ reads

$$\hbar\frac{d}{dt}\mathbf{C}(t) = -iH(t)\mathbf{C}(t), \tag{1}$$

where $\mathbf{C}(t)$ is the column-vector formed of $C_k(t)$.

The system is assumed to be initially in state ψ_1,

$$C_1(-\infty)=1,\quad C_k(-\infty)=0,\quad (k=2,\ ...,N), \tag{2}$$

and the quantities of interest are the populations,

$$P_k(t) = |C_k(t)|^2, \qquad (k=1,2,\ ...,N), \tag{3}$$

particularly their values $P_k(\infty)$ at $t\to+\infty$. We refer to the probability $P_N(\infty)$ as the *population transfer efficiency*.

The basic STIRAP procedure involves three (nondegenerate bound) states, driven by two interactions, as described by the rotating-wave approximation (RWA) Hamiltonian matrix,

$$H(t) = \frac{\hbar}{2}\begin{bmatrix} 0 & \Omega_P(t) & 0 \\ \Omega_P(t) & 2\Delta_P & \Omega_S(t) \\ 0 & \Omega_S(t) & 2\delta \end{bmatrix}. \tag{4}$$

The time-varying Rabi frequencies $\Omega_P(t)$ and $\Omega_S(t)$ are, in the simplest approach (involving, for example, single-photon transitions and the RWA), just products of dipole moments and electric field amplitudes, such as

$$\hbar\Omega_P(t) = -d_{12}\mathcal{E}_P(t), \qquad \hbar\Omega_S(t) = -d_{23}\mathcal{E}_S(t). \tag{5}$$

We have here chosen the phases and energy zero-point so that the first diagonal element vanishes, $H_{11}=0$. With this choice, the third diagonal element, the two-step detuning δ, is the difference between the detuning of the pump transition Δ_P and the Stokes transition Δ_S,

$$\delta = \Delta_P - \Delta_S. \tag{6}$$

The essence of the STIRAP procedure can be understood in the following way. The arrival of the Stokes pulse establishes the system in one of the three dressed eigenstates of the instantaneous Hamiltonian (4). This coherent superposition of atomic states is the so-called *trapped state*,

$$\varphi_T(t) = \frac{1}{\Omega(t)}\begin{bmatrix} \Omega_S(t) \\ 0 \\ -\Omega_P(t) \end{bmatrix} \tag{7}$$

where $\Omega(t) = \sqrt{|\Omega_S(t)|^2 + |\Omega_P(t)|^2}$ is the mean-square Rabi frequency. If, and only if, the two-photon detuning δ vanishes, this state is a null-eigenvalue eigenstate of the full Hamiltonian. By maintaining sufficiently slow variation of Rabi frequencies (a condition which amounts to requiring that the pulse areas be much larger than π), one can force the system to remain in the trapped state as the Stokes pulse is replaced by the pump pulse. At the end of the pair of pulses, when only the pump pulse acts, the trapped state coincides with the desired target state ψ_3 and population transfer has therefore been achieved. Moreover, since the trapped state (7) does not involve a contribution from the intermediate state ψ_2, the latter is not populated in the adiabatic limit and hence, its properties, including a possible decay to other states, do not affect the transfer efficiency.

2.2 Multistate extension

The basic idea of the present extension of STIRAP to chainwise-linked multistate systems with more than three states (following [33]) is as follows. We have a set of N unperturbed basis states, connected sequentially by $N-1$ laser pulses: a *pump* pulse $\Omega_P(t)$ (connecting states ψ_1 and ψ_2), a *Stokes* pulse $\Omega_S(t)$ (connecting states ψ_{N-1} and ψ_N), and *control* pulses $\Omega_C(t)$, which connect the intermediate states in a chainwise manner $\psi_2 \leftrightarrow \psi_3 \leftrightarrow \cdots \leftrightarrow \psi_{N-1}$. We require that the control pulses are strong and long compared with the pump and Stokes pulses so that they are nearly constant during the times when $\Omega_P(t)$ and $\Omega_S(t)$ are present. The N-state system is initially in state ψ_1 and we want to transfer the population to state ψ_N, as completely and selectively as possible, by passing the intermediate states.

The objective of the control pulses is to make the $N-2$ intermediate states act collectively as a physical object with properties reminiscent of those of the single intermediate state in the usual three-state STIRAP. We want to find the conditions (detunings and Rabi frequencies) which will make the excitation dynamics basically that of an effective three-state system.

In order to achieve this, we first carry out a preliminary diagonalization of the subsystem comprising the $N-2$ strongly coupled intermediate states. This gives us a set of $N-2$ *dressed* states. The transformed sub-Hamiltonian has two parts: an adiabatic part, containing the eigenenergies, and a diabatic part, containing the couplings between the dressed states. For *constant* control pulses (which is approximately the case during the times when $\Omega_P(t)$ and $\Omega_S(t)$ are present if the control pulses are very long), the diabatic part vanishes and the eigenenergies of the subsystem are constant. The transformation produces an effective N-state Hamiltonian, comprising $N-2$ superposed Λ transitions, in which state ψ_1 is coupled simultaneously to $N-2$ dressed states, all of which are coupled in turn to state ψ_N. We then tune the pump and Stokes frequencies to exact resonance with one of the dressed states. In this way, we are left with only three strongly coupled states: states ψ_1, ψ_N, and one resonant dressed state. These three states behave as do those of the standard (three-state) STIRAP system.

The condition for this three-state approximation is the vanishing of a dressed eigenvalue, which can be expressed as the vanishing of a submatrix determinant. We will demonstrate analytically and numerically that this choice produces the desired effect, namely good population transfer.

To understand why this works, we inspect the effective three-state Hamiltonian obtained by adiabatically eliminating all the nonresonant states. Then one has the usual three-state problem, except for an additional direct coupling between states ψ_1 and ψ_N, and additional diagonal elements which lead to an effective nonzero two-photon detuning between states ψ_1 and ψ_N. Both the nonzero detuning and the direct $\psi_1 \leftrightarrow \psi_N$ coupling are inversely proportional to an eigenvalue or some combination of eigenvalues, and thus, they will be negligible if the dressed eigenvalues are very different; this can be achieved by using *strong* control pulses. Hence, if all above conditions (strong and constant control pulses in addition to pump and Stokes pulses tuned to a dressed eigenstate) are met, we will have an effective three-state STIRAP process in our N-state ladder system.

In Section 3, we describe this scheme explicitly in the four-state case, which illustrates the generic properties of N-state systems and is the most likely candidate for experimental verification of our results. Then we consider the general N-state case in Section 4.

3 Four-state system

3.1 The four-state system

The four-state Hamiltonian in the RWA is given by the tridiagonal matrix

$$H(t) = \frac{\hbar}{2}\begin{bmatrix} 0 & \Omega_P(t) & 0 & 0 \\ \Omega_P(t) & 2\Delta_2 & \Omega_C & 0 \\ 0 & \Omega_C & 2\Delta_3 & \Omega_S(t) \\ 0 & 0 & \Omega_S(t) & 0 \end{bmatrix}. \tag{8}$$

We have here assumed, as is always possible with appropriate choice of phases and energy zero-point, that the first diagonal element vanishes. In analogy with STIRAP, we also suppose that the final diagonal element vanishes, *i.e.* that states ψ_1 and ψ_4 are on three-photon resonance. Furthermore, because the phases of the Ω's can always be attached to the probability amplitudes by an appropriate phase transformation, we shall, without loss of generality, take all Rabi frequencies to be real and positive. We assume that the pulses $\Omega_P(t)$ and $\Omega_S(t)$ are ordered counterintuitively ($\Omega_S(t)$ preceding $\Omega_P(t)$), while Ω_C is constant. In the numerical simulations we use

$$\Omega_P(t) = \Omega_0 f(t-\tau), \tag{9a}$$
$$\Omega_S(t) = \Omega_0 f(t+\tau), \tag{9b}$$
$$\Omega_C = \xi\Omega_0, \tag{9c}$$

where $f(t) = e^{-(t/T)^2}$ is a Gaussian pulse, τ mesures the time delay between Ω_P and Ω_S, and we take $\xi \gg 1$ in order to reduce the populations of the intermediate states [33].

3.2 Equivalent double-Λ system

A key result of the present work is the recognition that it is desirable to adjust the laser parameters in such a manner that one of the eigenstates of the (constant) Hamiltonian

$$H^{(i)} = \frac{\hbar}{2}\begin{bmatrix} 2\Delta_2 & \Omega_C \\ \Omega_C & 2\Delta_3 \end{bmatrix}, \tag{10}$$

which describes the strongly coupled intermediate states ψ_2 and ψ_3, is exactly on resonance. In other words, one of the eigenvalues of $H^{(i)}$ has to be zero. We then anticipate particularly robust population transfer between states ψ_1 and ψ_4 because this four-state system is equivalent to an on-resonance three-state system, used in the standard STIRAP, plus an additional intermediate state. The latter couples to states ψ_1 and ψ_4 but is detuned far off resonance and hence, its influence on the transfer process is negligible.

The (constant) transformation matrix, which casts our initial chainwise-linked system $\psi_1 \leftrightarrow \psi_2 \leftrightarrow \psi_3 \leftrightarrow \psi_4$ into the form of a double-Λ system $\psi_1 \Leftrightarrow \Phi_2, \Phi_3 \Leftrightarrow \psi_4$, is given by

$$W = \begin{bmatrix} 1 & 0 & 0 & 0 \\ 0 & c & s & 0 \\ 0 & -s & c & 0 \\ 0 & 0 & 0 & 1 \end{bmatrix},$$

where

$$c = \cos\vartheta, \qquad s = \sin\vartheta \tag{11}$$

and the (constant) rotation angle ϑ is defined by

$$\tan 2\vartheta = \frac{\Omega_C}{\Delta_3 - \Delta_2}, \qquad \left(0 < \vartheta < \frac{\pi}{2}\right).$$

The probability amplitudes in the two bases are related by $\mathbf{C} = W\mathbf{C}'$, where $\mathbf{C}'$ has the components $\{C_1, C_2', C_3', C_4\}$, C_k' being the amplitude of state Φ_k. The Hamiltonians are related by $H' = W^{-1}HW$, or explicitly,

$$H'(t) = \frac{\hbar}{2}\begin{bmatrix} 0 & \Omega_P(t)c & \Omega_P(t)s & 0 \\ \Omega_P(t)c & 2\eta_2 & 0 & -\Omega_S(t)s \\ \Omega_P(t)s & 0 & 2\eta_3 & \Omega_S(t)c \\ 0 & -\Omega_S(t)s & \Omega_S(t)c & 0 \end{bmatrix}, \quad (12)$$

where

$$\eta_{2,3} = \frac{1}{2}\left[\Delta_2 + \Delta_3 \mp \sqrt{(\Delta_2+\Delta_3)^2 + \Omega_C^2 - 4\Delta_2\Delta_3}\right] \quad (13)$$

are the eigenvalues of $H^{(i)}/\hbar$. The subscripts for η_2 and η_3 are chosen to comply with the notation in the general N-state case (Sect. 4). Because W is constant, the Schrödinger equation in the new basis reads

$$\hbar\frac{d}{dt}\mathbf{C}'(t) = -iH'(t)\mathbf{C}'(t). \quad (14)$$

We point out that it is *exact* as long as Ω_C is constant. If Ω_C were time-dependent (*e.g.* pulse-shaped), H' would include a term $-i\hbar W^{-1}\dot{W}$ and there would be a nonzero coupling between states Φ_2 and Φ_3. As equation (12) shows, for a constant Ω_C there is no such coupling. This equivalent four-state system, comprising two superposed parallel Λ-transitions, is shown schematically in Figure 1b, where it can be contrasted with the original four-state system of Figure 1a.

3.3 Tuning to a dressed state

Obviously, one of the eigenvalues (13) will be equal to zero if

$$\Omega_C^2 = 4\Delta_2\Delta_3. \quad (15)$$

There are two possibilities: if $\Delta_2 > 0$ and $\Delta_3 > 0$, we have $\eta_3 = \Delta_2 + \Delta_3$ and $\eta_2 = 0$, while if $\Delta_2 < 0$ and $\Delta_3 < 0$ we have $\eta_2 = \Delta_2 + \Delta_3$ and $\eta_3 = 0$. There is no physical mechanism favoring either of these two cases. This is particularly transparent if we notice that the population dynamics is invariant with respect to the simultaneous change of sign of Δ_2 and Δ_3, which is a general property of equation (1). Furthermore, given condition (15), we still have the freedom to choose the values of Δ_2 and Δ_3. The most reasonable choice seems to be $\Delta_2 \approx \Delta_3$ because then $\vartheta = \frac{1}{4}\pi$ and the couplings of states Φ_2 and Φ_3 to state ψ_1 are of the same order as the couplings of states Φ_2 and Φ_3 to state ψ_4 (see Eq. (12)). A great difference between Δ_2 and Δ_3 would lead to an imbalance in these couplings and consequent lowering of transfer efficiency. Moreover, $\Delta_2 = \Delta_3$ means that the control laser is on resonance with the $\Phi_2 \leftrightarrow \Phi_3$ transition, which maximizes the coupling between them.

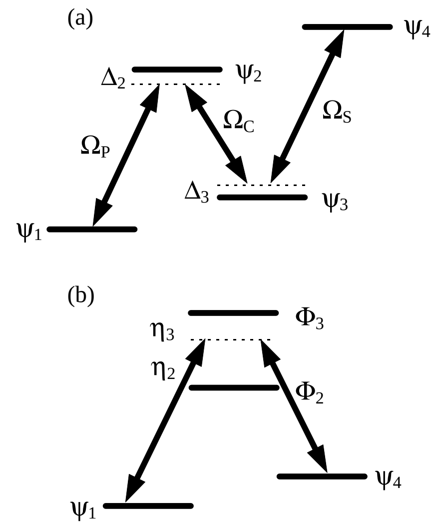

Fig. 1. (a) The chainwise-linked four-state system studied in Section 3. (b) The equivalent four-state system which consists of states ψ_1 and ψ_4 plus two intermediate states Φ_2 and Φ_3. Each intermediate state is coupled to state ψ_1 with a coupling proportional to Ω_P and to state ψ_4 with a coupling proportional to Ω_S. The intermediate states Φ_2 and Φ_3 are detuned from resonance with detunings of η_2 and η_3 while states ψ_1 and ψ_4 are on two-photon resonance.

As has been pointed out in [40], a necessary condition for STIRAP-like population transfer in multistate systems is the existence of an adiabatic-transfer (AT) state $\varphi_T(t)$, *i.e.*, of an eigenstate of $H(t)$ having the property

$$\varphi_T(t) = \begin{cases} \psi_1, & t \to -\infty \\ \psi_N, & t \to +\infty \end{cases}. \quad (16)$$

This state generalizes the trapped state (7) in STIRAP. For our four-state system, the condition for existence of state $\varphi_T(t)$ is [40]

$$\Delta_2\Delta_3 > 0. \quad (17)$$

This condition has earlier been derived subject to the assumption that $4\Delta_2\Delta_3 \neq \Omega_C^2$ [40], which is exactly opposite to the tuning-to-eigenvalue condition (15). We show in Appendix that for *arbitrary* number of states, state $\varphi_T(t)$ always exists when the pump and Stokes lasers are tuned to any of the eigenstates of the intermediate subsystem. We note in passing that condition (17) is always fulfilled when condition (15) is fulfilled, which means that in the (Δ_2, Δ_3)-plane, the tuning-to-eigenvalue curves, defined by (15), lie *within* the AT regions, defined by (17). This also means that relation (17) provides the necessary and sufficient condition for existence of the AT state in all cases, including when $4\Delta_2\Delta_3 = \Omega_C^2$.

3.4 Effective three-state problem

3.4.1 Adiabatic elimination of the off-resonant dressed state

Provided the intermediate coupling Ω_C is strong (*i.e.* $\xi \gg 1$) and condition (15) is approximately fulfilled, we can adiabatically eliminate the off-resonant eigenstate. To be specific, suppose that Δ_2 and Δ_3 are both positive. Then we have $|\eta_2| \ll \eta_3$ and we can eliminate state Φ_3. We set $\dot{C}'_3 = 0$ in equation (14), find C'_3 from the resulting algebraic equation in terms of C_1 and C_4, and then replace it in the first and fourth equations. As a result, we obtain an effective three-state description,

$$\hbar \frac{d}{dt}\mathbf{C}^{(eff)} = -iH^{(eff)}\mathbf{C}^{(eff)}, \tag{18}$$

where $\mathbf{C}^{(eff)} = (C_1, C'_2, C_4)^T$ and

$$H^{(eff)} = \frac{\hbar}{2}\begin{bmatrix} -\Omega_P^2 s^2/2\eta_3 & \Omega_P c & -\Omega_P\Omega_S sc/2\eta_3 \\ \Omega_P c & 2\eta_2 & -\Omega_S s \\ -\Omega_P\Omega_S sc/2\eta_3 & -\Omega_S s & -\Omega_S^2 c^2/2\eta_3 \end{bmatrix}, \tag{19}$$

with c and s defined by equations (11) (we have here omitted arguments showing the explicit time dependence of $H^{(eff)}$, Ω_P and Ω_S). The effect of the adiabatically eliminated state Φ_3 on the effective three-state system appears as a nonzero two-photon detuning and as a direct coupling between states ψ_1 and ψ_4. Both of these changes can be expected to reduce the transfer efficiency as compared to the standard three-state STIRAP. This negative effect is decreased when Ω_C is large: then Δ_2 and Δ_3 are also large (because of (15)) and hence, η_3 is large too, which reduces the effective two-photon detuning and the $\psi_1 \leftrightarrow \psi_4$ coupling. Note that we have allowed for some deviation from the tuning-to-resonance condition (15), *i.e.* we allow a nonzero η_2, in order to be able to examine (in Sect. 3.4.3) the effects of the deviation from exact resonance.

3.4.2 Existence of adiabatic-transfer state

The equation for the eigenvalues of the effective three-state (time-dependent) Hamiltonian (19) reads $\det(H^{(eff)}/\hbar - \mu 1) = 0$, or explicitly,

$$\begin{aligned}&16\eta_3\mu^3 + 4\left(\Omega_P^2 s^2 + \Omega_S^2 c^2 - 4\eta_2\eta_3\right)\mu^2 \\ &-4\left[\eta_2\left(\Omega_P^2 s^2 + \Omega_S^2 c^2\right) + \eta_3\left(\Omega_P^2 c^2 + \Omega_S^2 s^2\right)\right]\mu \\ &-\Omega_P^2\Omega_S^2 = 0.\end{aligned} \tag{20}$$

Unlike conventional STIRAP, there is *no* zero eigenvalue for $\Omega_P \neq 0$ and $\Omega_S \neq 0$. The implication is that the intermediate state *is* populated during the transfer. This fact, along with the extra two-photon detuning and the direct $\psi_1 \leftrightarrow \psi_4$ coupling, mean that the effective three-state problem (18) *differs* from the standard STIRAP. We will show, however, that when $\eta_2 = 0$ (and hence, condition (15) is fulfilled), it is similar to STIRAP and allows for complete STIRAP-like population transfer.

First, we need to find the eigenvalues from equation (20). They can be found exactly [1] but the precise expressions are not needed for the present analysis. We have only to determine their asymptotic behaviors at large negative and positive times. As equation (20) shows, for $\eta_2 = 0$ all three eigenvalues vanish as $t \to \pm\infty$ because then both Ω_P and Ω_S vanish. Furthermore, when either Ω_P or Ω_S is nonzero and the other is zero, there is only one zero eigenvalue. Hence, when the Stokes pulse Ω_S arrives, the degeneracy of two of the eigenvalues, μ_1^- and μ_2^-, is lifted and they depart from zero. The third eigenvalue μ_0^- stays zero until the pump pulse Ω_P arrives later.

To find how μ_0^- departs from zero with Ω_P, we differentiate equation (20) with respect to Ω_P^2, set $\Omega_P^2 = 0$ and $\mu_0^- = 0$ and find $(d\mu_0^-/d\Omega_P^2)_{\Omega_P^2=0}$. By using the Taylor expansion of μ_0^- against Ω_P^2, we obtain

$$\mu_0^- \approx -\frac{\Omega_P^2}{4\eta_3 s^2}\cdot \tag{21}$$

The other two eigenvalues can be found by setting $\Omega_P = 0$ in equation (20) and dividing by μ (which accounts for removing the root μ_0^-). Accounting for $|\eta_3| \gg \Omega_P, \Omega_S$, we find

$$\mu_1^- \approx -\frac{1}{2}\Omega_S s, \quad \mu_2^- \approx \frac{1}{2}\Omega_S s. \tag{22}$$

In a similar manner, we find that as $t \to +\infty$, the eigenvalues have the following asymptotic behavior

$$\mu_0^+ \approx -\frac{\Omega_S^2}{4\eta_3 c^2}, \quad \mu_1^+ \approx -\frac{1}{2}\Omega_P c, \quad \mu_2^+ \approx \frac{1}{2}\Omega_P c. \tag{23}$$

Since $\Omega_P/\Omega_S \to 0$ as $t \to -\infty$ and $\Omega_S/\Omega_P \to 0$ as $t \to +\infty$, the relations $\mu_1^- < \mu_0^- < \mu_2^-$ and $\mu_1^+ < \mu_0^+ < \mu_2^+$ hold. Hence, insofar as the eigenvalues do not cross, the linkages $\mu_0^- \leftrightarrow \mu_0^+$, $\mu_1^- \leftrightarrow \mu_1^+$, and $\mu_2^- \leftrightarrow \mu_2^+$ take place. It can readily be shown that at large negative times, the eigenstate corresponding to μ_0^- is equal to state ψ_1, while those corresponding to μ_1^- and μ_2^- are equal to superpositions of states Φ_2 and ψ_4. At large positive times, the eigenstate corresponding to μ_0^+ is equal to state ψ_4, while those corresponding to μ_1^+ and μ_2^+ are equal to superpositions of states ψ_1 and Φ_2. Hence, the eigenstate, whose eigenvalue tends to μ_0^- initially and to μ_0^+ finally, is an adiabatic-transfer state, as defined by equation (16), and it transfers the population from state ψ_1 to state ψ_4 in the adiabatic limit. In this sense, this eigenstate is similar to the trapped state (7), but unlike the trapped state, it involves a contribution from the intermediate state Φ_2. Finally, we note that for simplicity, the above results for $\mu_1^\pm$ and $\mu_2^\pm$ have been derived upon the assumption that $|\eta_3| \gg \Omega_P, \Omega_S$. Without this assumption, the corresponding expressions are slightly more complicated but the connectivity conclusions remain valid.

3.4.3 Adiabaticity

We will show that tuning to a subsystem eigenvalue optimizes adiabaticity because it maximizes the separation between the AT eigenvalue and the other two eigenvalues. For the sake of simplicity, we will only consider the eigenvalues at $t = 0$, where the overlap between the pump

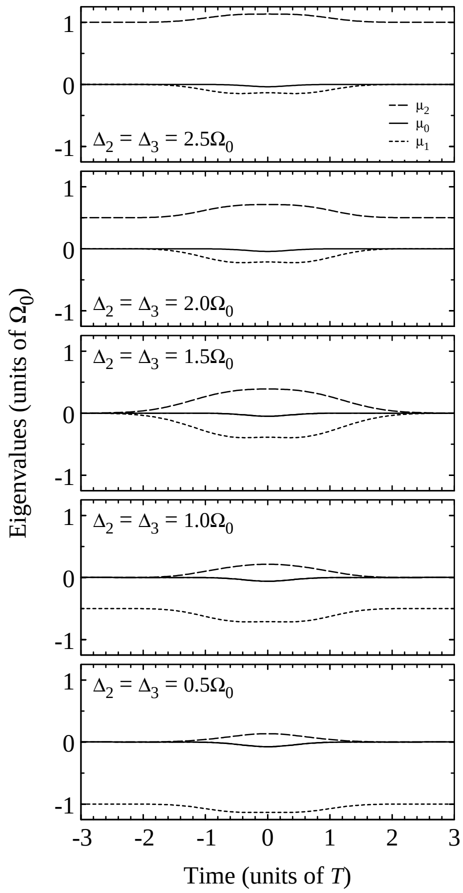

Fig. 2. The time evolutions of the eigenvalues μ_0 (solid curve), μ_1 (short-line dashed curve), and μ_2 (long-line dashed curve) (the roots of Eq. (20)), plotted for five different values of the detunings $\Delta_2 = \Delta_3 \equiv \Delta$. The pulse shapes are given by equations (9) with $f(t) = e^{-(t/T)^2}$, $T = \Omega_0^{-1}$, and $\tau = 0.5T$. The relative strength of the control pulse is $\xi = 3$.

and Stokes pulses is maximal. According to our assumption (9), at $t = 0$ we have $\Omega_P = \Omega_S$. Then the roots of equation (20) are exactly given by the expressions

$$\mu_{1,2} = \frac{1}{2}\left(\eta_2 \mp \sqrt{\eta_2^2 + \Omega_P^2}\right), \tag{24a}$$

$$\mu_0 = -\frac{\Omega_P^2}{4\eta_3}, \tag{24b}$$

with $\eta_{2,3}$ defined by equation (13). Obviously, $\mu_1 < \mu_0 < 0 < \mu_2$. Without losing much generality we furthermore suppose that $\Delta_2 = \Delta_3 \equiv \Delta$; then $\eta_{2,3} = \Delta \mp \frac{1}{2}\Omega_C$. Both μ_1 and μ_2 are increasing functions of η_2 and hence, of Δ. Moreover, μ_0 too increases with Δ and tends to zero at large Δ. Furthermore, for large negative η_2 ($\Delta < \frac{1}{2}\Omega_C$), $\mu_1 \to \eta_2$ and $\mu_2 \to 0$, whereas for large positive η_2 ($\Delta > \frac{1}{2}\Omega_C$), $\mu_1 \to 0$ and $\mu_2 \to \eta_2$. This means that if we fix all Rabi frequencies and increase Δ, μ_1 will approach μ_0 from below, while μ_2 will move upwards and away from μ_0. These features are clearly seen in Figure 2, where the time evolutions of the three eigenvalues μ_0, μ_1, and μ_2 (the roots of Eq. (20)), are plotted for five different values of the detunings $\Delta_2 = \Delta_3 \equiv \Delta$. The pulse shapes are given by equations (9) with $f(t) = e^{-(t/T)^2}$, $T = \Omega_0^{-1}$, and $\tau = 0.5T$. The relative strength of the control pulse is kept the same, $\xi = 3$.

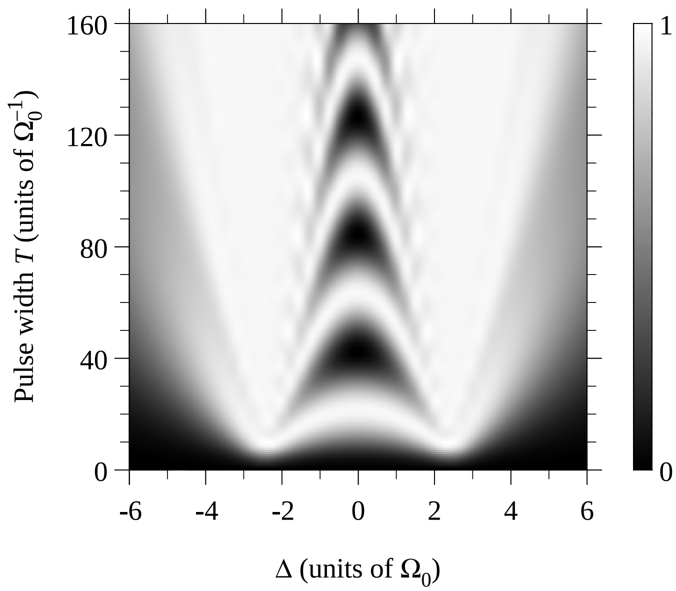

Fig. 3. The population P_4 in a four-state system for the pulses given in equation (9) against the pulse width T and the detuning $\Delta \equiv \Delta_2 = \Delta_3$, obtained by numerical solution of the Schrödinger equation. The other parameters are $\tau = 0.5T$, $\Omega_C = 5\Omega_0$.

Inasmuch as adiabaticity is most significantly affected by the eigenvalue which is closest to μ_0, the optimal case is when μ_1 and μ_2 are equally separated from μ_0, *i.e.* $\mu_2 - \mu_0 = \mu_0 - \mu_1$. This takes place for $\Delta = \Delta_o$, where

$$\Delta_o = \frac{1}{2}\sqrt{\Omega_C^2 - 2\Omega_P^2} \approx \frac{1}{2}\Omega_C - \frac{\Omega_P^2}{2\Omega_C}\,. \tag{25}$$

In the last approximation we have used the constraint $\Omega_P \ll \Omega_C$. For $\Delta < \Delta_o$, the eigenvalue μ_2 is closer to μ_0, while for $\Delta > \Delta_o$, it is the eigenvalue μ_1 that approaches μ_0. Condition (25) shows that the tuning-to-eigenvalue condition (15) provides the detunings that ensure nearly the best adiabaticity. The small difference between conditions (15) and (25) is due to the peculiar behavior of μ_1 near $t = 0$, where it has a local maximum. It can be shown, after some algebra, that the above conclusions remain valid for $t \neq 0$ as well. Finally, it should be noted that the same estimate as (25) can be obtained from the full four-state Hamiltonian (8) by using the exact expressions for the four eigenvalues derived in [40].

In Figure 3, we have plotted the final-state population P_4 for the pulses given in equations (9) *versus* the pulse width T and the detuning $\Delta \equiv \Delta_2 = \Delta_3$. The other parameters are $\tau = 0.5T$ and $\xi = 5$ (*i.e.* $\Omega_C = 5\Omega_0$). In this figure, regions of high population transfer appear white, whereas regions of low transfer appear dark. As T increases, the adiabatic limit is approached. The figure is symmetric with respect to the sign of Δ because the populations are invariant upon the simultaneous change of sign of the detunings. We note that for $\Delta_2 = \Delta_3 \equiv \Delta$, as we assume, equation (15) gives the condition for tuning to resonance as $\Delta = \pm\frac{1}{2}\xi\Omega_0$. For the choice of parameters of the figure ($\xi = 5$) the condition is $\Delta = \pm 2.5\Omega_0$. In confirmation of this result, we see that the regions close to $\Delta = \pm 2.5\Omega_0$ ensure the best transfer conditions, that is, the adiabatic limit $P_4 \approx 1$ is reached most quickly (as T increases) and there are virtually no oscillations. This shows that the STIRAP-like process works best with the "tuning-to-eigenvalue" approach, although it can work in principle for other values of Δ (because an AT state exists for any $\Delta \neq 0$ in this particular case). The difference is *how quickly* the adiabatic limit is approached. This happens most quickly for $\Delta = \pm 2.5\Omega_0$ where $\Delta_2\Delta_3 = \frac{1}{4}\Omega_C^2$. Near $\Delta = 0$, the final-state population oscillates, in agreement with the conclusions in [31,32,40].

3.5 Intermediate-state populations

We now return to the original four-state problem. In order to estimate the intermediate-state populations P_2 and P_3, we need the AT eigenvalue $\lambda_T(t)$ and the corresponding AT eigenstate $\varphi_T(t)$, the exact expressions for which are too complicated to show here. It has been shown elsewhere [40] that at $t = 0$, where the overlap between the pump and Stokes pulse is maximal, the populations of states ψ_2 and ψ_3 are exactly given by

$$P_2(0) = P_3(0) = \frac{1}{2 + \frac{1}{2}[\Omega_P(0)/\lambda_T(0)]^2}, \tag{26}$$

where

$$\lambda_T(0) = \frac{1}{2}\left[\Delta + \frac{1}{2}\Omega_C - \sqrt{\left(\Delta + \frac{1}{2}\Omega_C\right)^2 + \Omega_P^2(0)}\right], \tag{27}$$

We assume that $\Omega_P(0) = \Omega_S(0)$, which is the case for the pulse shapes (9), and that $\Delta_2 = \Delta_3 \equiv \Delta > 0$. Although the maxima of $P_2(t)$ and $P_3(t)$ are not at $t = 0$, equation (26) provides values close to the maximal ones, particularly for the total population in the intermediate states, $P_2(t)+P_3(t)$. As $\Delta + \frac{1}{2}\Omega_C$ increases, equations (26, 27) show that λ_T decreases, and so do $P_2(t)$ and $P_3(t)$. For $\Delta + \frac{1}{2}\Omega_C \gg \Omega_P(0)$, this happens in a Lorentzian manner,

$$P_2(0) = P_3(0) \approx \frac{1}{2 + 8(\Delta + \frac{1}{2}\Omega_C)^2/\Omega_P^2(0)}\cdot \tag{28}$$

Equations (26, 28) show that tuning to a dressed eigenstate has no strong effect upon decreasing the intermediate-state populations, for which it is only important that the sum $\Delta + \frac{1}{2}\Omega_C$ is large. The significance of the tuning-to-resonance choice $\Delta = \frac{1}{2}\Omega_C$, as we found in Section 3.4.3, shows up in maximizing the separations between the AT eigenvalue and its neighbors, thereby giving the most adiabatic evolution. Hence, we can keep the final-state population relatively unaffected and still damp the intermediate populations by increasing *both* Δ and Ω_C, while maintaining the tuning condition (17).

4 N-state system

We turn now to the general case of N-state system, involving $N-2$ intermediate states coupled by constant control pulses. The analysis extends the case $N = 4$ just presented.

4.1 An equivalent multi-Λ system

The RWA Hamiltonian of an N-state chainwise-linked system,

$$H = \frac{\hbar}{2}\begin{bmatrix} 0 & \Omega_{1,2} & 0 & \cdots & 0 & 0 \\ \Omega_{1,2} & 2\Delta_2 & \Omega_{2,3} & \cdots & 0 & 0 \\ 0 & \Omega_{2,3} & 2\Delta_3 & \cdots & 0 & 0 \\ \vdots & \vdots & \vdots & \ddots & \vdots & \vdots \\ 0 & 0 & 0 & \cdots & 2\Delta_{N-1} & \Omega_{N-1,N} \\ 0 & 0 & 0 & \cdots & \Omega_{N-1,N} & 0 \end{bmatrix}, \tag{29}$$

can be transformed to an equivalent representation which provides useful insight into the dynamics when the intermediate couplings are strong. The desired transformation replaces the $N-2$ intermediate states of the original system with the eigenstates $\Phi_2, \Phi_3, \ldots, \Phi_{N-1}$ of the Hamiltonian $H^{(i)}$, which describes only the intermediate states and the couplings between them and is given by the submatrix from element $(2,2)$ to $(N-1, N-1)$ of H. The diagonalization of this sub-Hamiltonian,

$$\left[W^{(i)}\right]^{-1} H^{(i)} W^{(i)} = \hbar\eta, \tag{30}$$

is carried out by the orthogonal matrix $W^{(i)}$ whose columns are the normalized eigenvectors Φ_k of $H^{(i)}$, $\Phi_k = \left[v_2^{(k)}, v_3^{(k)}, \ldots, v_{N-1}^{(k)}\right]^T$, for $k = 2, 3, \ldots, N-1$. The diagonal matrix $\hbar\eta$ contains on its main diagonal the eigenvalues $\hbar\eta_2, \hbar\eta_3, \ldots, \hbar\eta_{N-1}$ of $H^{(i)}$.

The transformation of the full Hamiltonian H is carried out by the $N \times N$ real orthogonal matrix

$$W = \begin{bmatrix} 1 & 0 & 0 & \cdots & 0 & 0 & 0 \\ 0 & v_2^{(2)} & v_2^{(3)} & \cdots & v_2^{(N-2)} & v_2^{(N-1)} & 0 \\ 0 & v_3^{(2)} & v_3^{(3)} & \cdots & v_3^{(N-2)} & v_3^{(N-1)} & 0 \\ \vdots & \vdots & \vdots & \ddots & \vdots & \vdots & \vdots \\ 0 & v_{N-2}^{(2)} & v_{N-2}^{(3)} & \cdots & v_{N-2}^{(N-2)} & v_{N-2}^{(N-1)} & 0 \\ 0 & v_{N-1}^{(2)} & v_{N-1}^{(3)} & \cdots & v_{N-1}^{(N-2)} & v_{N-1}^{(N-1)} & 0 \\ 0 & 0 & 0 & \cdots & 0 & 0 & 1 \end{bmatrix}. \tag{31}$$

The probability amplitudes in the original and the transformed bases are related as $\mathbf{C} = W\mathbf{C}'$, where the column-vector $\mathbf{C}'$ has as elements the amplitudes $\{C_1, C_2', C_3', \ldots, C_{N-1}', C_N\}$, C_k' being the amplitude of the dressed state Φ_k. The Schrödinger equation in the new basis reads

$$\hbar\frac{d}{dt}\mathbf{C}' = -iH'\mathbf{C}', \tag{32}$$

where the transformed Hamiltonian is

$$H' = W^{-1}HW - i\hbar W^{-1}\frac{d}{dt}W. \qquad (33)$$

The first part of this expression, $W^{-1}HW$, describes a multi-Λ system (as can be seen from the explicit form below). When the couplings $\Omega_{2,3}, \Omega_{3,4}, \ldots, \Omega_{N-2,N-1}$ between the bare intermediate states in the original chain system depend on time (are pulsed), the derivative term on the right-hand side of equation (33) introduces couplings between the dressed states $\Phi_2, \Phi_3, \ldots, \Phi_{N-1}$. For *constant* intermediate couplings, the derivative is zero and the dressed states are uncoupled. Then $H' = W^{-1}HW$, or explicitly,

$$H' = \frac{\hbar}{2}\begin{bmatrix} 0 & \Omega_P v_2^{(2)} & \Omega_P v_2^{(3)} & \cdots & \Omega_P v_2^{(N-1)} & 0 \\ \Omega_P v_2^{(2)} & 2\eta_2 & 0 & \cdots & 0 & \Omega_S v_{N-1}^{(2)} \\ \Omega_P v_2^{(3)} & 0 & 2\eta_3 & \cdots & 0 & \Omega_S v_{N-1}^{(3)} \\ \vdots & \vdots & \vdots & \ddots & \vdots & \vdots \\ \Omega_P v_2^{(N-1)} & 0 & 0 & \cdots & 2\eta_{N-1} & \Omega_S v_{N-1}^{(N-1)} \\ 0 & \Omega_S v_{N-1}^{(2)} & \Omega_S v_{N-1}^{(3)} & \cdots & \Omega_S v_{N-1}^{(N-1)} & 0 \end{bmatrix}. \qquad (34)$$

As in the four-state case, we have denoted $\Omega_{1,2} \equiv \Omega_P$ and $\Omega_{N-1,N} \equiv \Omega_S$.

The Hamiltonian H' describes an N-state system which consists of states ψ_1 and ψ_N plus $N-2$ dressed intermediate states $\Phi_2, \Phi_3, \ldots, \Phi_{N-1}$, each intermediate state being coupled to state ψ_1 with a coupling proportional to Ω_P and to state ψ_N with a coupling proportional to Ω_S. Each intermediate state is detuned from resonance with a detuning of η_k while states ψ_1 and ψ_N are on two-photon resonance. The new system can be viewed as $N-2$ simultaneous superposed two-photon Λ-transitions between states ψ_1 and ψ_N, thus generalizing the two parallel Λ-transitions depicted in Figure 1b.

Tuning to an eigenvalue of the sub-Hamiltonian $H^{(i)}$ will take place if the laser parameters are chosen so that

$$\mathcal{D}^{(2,N-1)} \equiv \det(H^{(i)}/\hbar) = 0, \qquad (35)$$

which indicates the existence of a zero eigenvalue of $H^{(i)}$. We shall refer to equation (35) as the *tuning-to-eigenvalue condition*. For $N = 4$, we have $\det(H^{(i)}/\hbar) = \Delta_2\Delta_3 - \frac{1}{4}\Omega_C^2$, and condition (35) reduces to condition (15), as it should. Given that the tuning condition (35) is fulfilled, one can again, as in the four-state case, by adiabatically eliminating the off-resonant dressed states reduce the N-state system to an effective three-state one, involving the strongly coupled initial state ψ_1, the final state ψ_N and the resonant intermediate state. At this stage, it is hard to recognize whether tuning to any particular eigenvalue of $H^{(i)}$ will be advantageous compared to tuning to another one. We shall return to this problem in Section 4.5.

4.2 Dressed eigenvalues

It can be verified after some algebra that if all intermediate Rabi frequencies are equal, $\Omega_{k,k+1} \equiv \Omega$ ($k = 2, 3, \ldots, N-2$), and if all intermediate detunings are equal too, $\Delta_k \equiv \Delta$ ($k = 2, 3, \ldots, N-1$), then the eigenvalues η_k are exactly given by

$$\eta_k = \Delta - \Omega\cos\frac{(k-1)\pi}{N-1}, \qquad (k = 2, 3, \ldots, N-1). \qquad (36)$$

Hence, the $N-2$ values of the detunings, for which the pump and Stokes lasers are tuned to a certain dressed state ($\eta_k = 0$), are given by the formula

$$\Delta^{(k)} = \Omega\cos\frac{(k-1)\pi}{N-1}, \qquad (k = 2, 3, \ldots, N-1). \qquad (37)$$

Because $\cos(x) = -\cos(\pi - x)$, these values are situated symmetrically on both sides of zero. Equation (36) shows that the eigenvalues increase (linearly) with the intermediate couplings, as do the separations between the eigenvalues. Consequently, our N-state system exhibits increasingly three-state behavior as the intermediate couplings increase. This feature remains valid for unequal intermediate couplings and detunings as well.

4.3 Adiabatic-transfer state

We show in Appendix that if condition (35) is fulfilled, one of the eigenstates of H is an adiabatic-transfer state, as defined by equation (16). In the general case of *arbitrary* laser parameters, an AT state may or may not exist. It has been shown elsewhere [40] that the condition for its existence reads

$$\mathcal{D}^{(2,N-2)}\mathcal{D}^{(3,N-1)} > 0, \qquad (38)$$

where $\mathcal{D}^{(j,k)}$ denotes the determinant $\mathcal{D}^{(j,k)}(\lambda)$, equation (A.2), estimated at $\lambda = 0$. This is the determinant of the square matrix obtained from $H/\hbar$ by keeping its columns from jth to kth and its rows from jth to kth as well. Condition (38) has earlier been derived under the assumption that $\mathcal{D}^{(2,N-1)} \neq 0$ [40]. The present derivation in the case when $\mathcal{D}^{(2,N-1)} = 0$ fills this gap. Moreover, as follows immediately from equations (A.12, A.13), the fulfillment of the tuning-to-eigenvalue condition (35) ensures the fulfillment of the AT condition (38). We shall see from the numerical simulations in the next subsection that the tuning to an eigenvalue of $H^{(i)}$ not only ensures the existence of the AT state but also *optimizes* the population transfer.

4.4 Examples

In Table 1, the condition for existence of the adiabatic-transfer state (38) and the tuning-to-eigenvalue condition

Table 1. The condition (38) for existence of an adiabatic-transfer state and the tuning-to-eigenvalue condition (35) given explicitly for four-, five-, six-, and seven-state systems.

N	AT condition (38)	Tuning condition (35)
4	$\Delta_2\Delta_3 > 0$	$4\Delta_2\Delta_3 = \Omega_{2,3}^2$
5	$\left(4\Delta_2\Delta_3 - \Omega_{2,3}^2\right)\left(4\Delta_3\Delta_4 - \Omega_{3,4}^2\right) > 0$	$4\Delta_2\Delta_3\Delta_4 = \Omega_{2,3}^2\Delta_4 + \Omega_{3,4}^2\Delta_2$
6	$\left(4\Delta_2\Delta_3\Delta_4 - \Omega_{2,3}^2\Delta_4 - \Omega_{3,4}^2\Delta_2\right)$ $\times\left(4\Delta_3\Delta_4\Delta_5 - \Omega_{3,4}^2\Delta_5 - \Omega_{4,5}^2\Delta_3\right) > 0$	$\left(4\Delta_2\Delta_3 - \Omega_{2,3}^2\right)\left(4\Delta_4\Delta_5 - \Omega_{4,5}^2\right) = 4\Delta_2\Delta_5\Omega_{3,4}^2$
7	$\left[\left(4\Delta_2\Delta_3 - \Omega_{2,3}^2\right)\left(4\Delta_4\Delta_5 - \Omega_{4,5}^2\right) - 4\Delta_2\Delta_5\Omega_{3,4}^2\right]$ $\times\left[\left(4\Delta_3\Delta_4 - \Omega_{3,4}^2\right)\left(4\Delta_5\Delta_6 - \Omega_{5,6}^2\right) - 4\Delta_3\Delta_6\Omega_{4,5}^2\right] > 0$	$\left(4\Delta_2\Delta_3\Delta_4 - \Omega_{2,3}^2\Delta_4 - \Omega_{3,4}^2\Delta_2\right)\left(4\Delta_5\Delta_6 - \Omega_{5,6}^2\right)$ $= \Omega_{4,5}^2\Delta_6\left(4\Delta_2\Delta_3 - \Omega_{2,3}^2\right)$

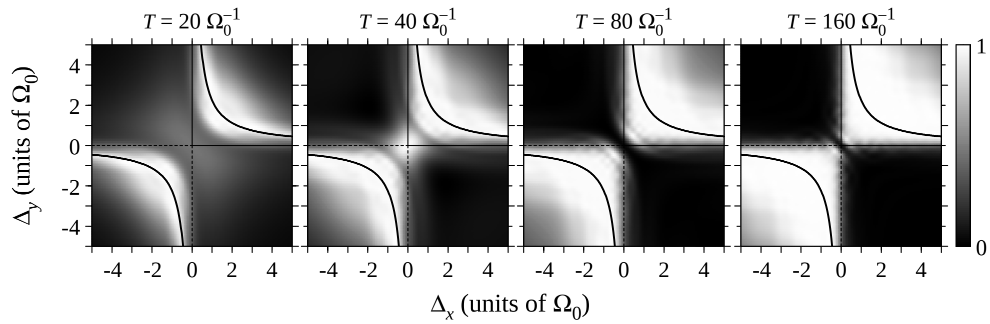

Fig. 4. The final-state population P_4 in a *four-state system*, obtained by numerical solution of the Schrödinger equation, plotted as a function of two detunings, Δ_x and Δ_y, where $\Delta_x \equiv \Delta_2$ and $\Delta_y \equiv \Delta_3$. The curves in the (Δ_x, Δ_y)-plane, on which the tuning-to-eigenvalue condition (35) is fulfilled, are shown by thick lines. The borders of the regions where the condition (38) for existence of an adiabatic-transfer state is fulfilled, are shown by thin solid or dashed lines. In all cases we have chosen the Rabi frequencies of the laser fields to be given by equations (9) and all intermediate Rabi frequencies to be equal to $\Omega_C = 3\Omega_0$. The four plots correspond to different characteristic pulse widths T.

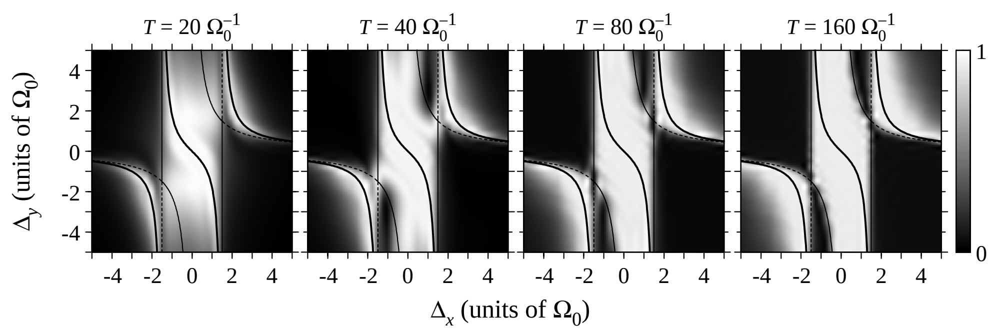

Fig. 5. The final-state population P_5 in a *five-state system*, obtained by numerical solution of the Schrödinger equation, plotted as a function of two detunings, Δ_x and Δ_y, where $\Delta_x \equiv \Delta_2 = \Delta_3$ and $\Delta_y \equiv \Delta_4$. The curves in the (Δ_x, Δ_y)-plane, on which the tuning-to-eigenvalue condition (35) is fulfilled, are shown by thick lines. The borders of the regions where the condition (38) for existence of an adiabatic-transfer state is fulfilled, are shown by thin solid or dashed curves. In all cases we have chosen the Rabi frequencies of the laser fields to be given by equations (9) and all intermediate Rabi frequencies to be equal to $\Omega_C = 3\Omega_0$. The four plots correspond to different characteristic pulse widths T.

(35) are given explicitly for four-, five-, six-, and seven-state systems.

We have solved the Schrödinger equation numerically for $N = 4$, 5, 6, and 7 states. Figures 4, 5, 6, and 7 present the final-state population P_N (the transfer efficiency) as grey-scale plots with $P_N = 1$ shown by white and $P_N = 0$ by black. In each of these figures we have plotted P_N as a function of two detunings, Δ_x and Δ_y, where

$$\begin{aligned}
&\text{for } N = 4: \Delta_x \equiv \Delta_2, && \Delta_y \equiv \Delta_3;\\
&\text{for } N = 5: \Delta_x \equiv \Delta_2 = \Delta_3, && \Delta_y \equiv \Delta_4;\\
&\text{for } N = 6: \Delta_x \equiv \Delta_2 = \Delta_3, && \Delta_y \equiv \Delta_4 = \Delta_5;\\
&\text{for } N = 7: \Delta_x \equiv \Delta_2 = \Delta_3 = \Delta_4, && \Delta_y \equiv \Delta_5 = \Delta_6.
\end{aligned}$$

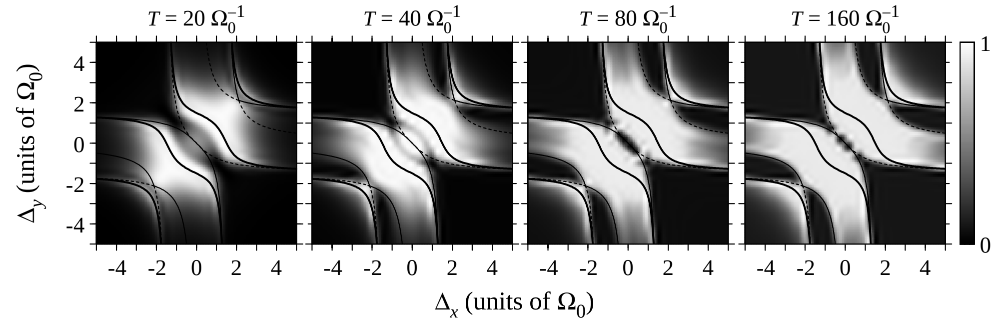

Fig. 6. The final-state population P_6 in a *six-state system*, obtained by numerical solution of the Schrödinger equation, plotted as a function of two detunings, Δ_x and Δ_y, where $\Delta_x \equiv \Delta_2 = \Delta_3$ and $\Delta_y \equiv \Delta_4 = \Delta_5$. The curves in the ($\Delta_x$, Δ_y)-plane, on which the tuning-to-eigenvalue condition (35) is fulfilled, are shown by thick lines. The borders of the regions where the condition (38) for existence of an adiabatic-transfer state is fulfilled, are shown by thin solid or dashed curves. In all cases we have chosen the Rabi frequencies of the laser fields to be given by equations (9) and all intermediate Rabi frequencies to be equal to $\Omega_C = 3\Omega_0$. The four plots correspond to different characteristic pulse widths T.

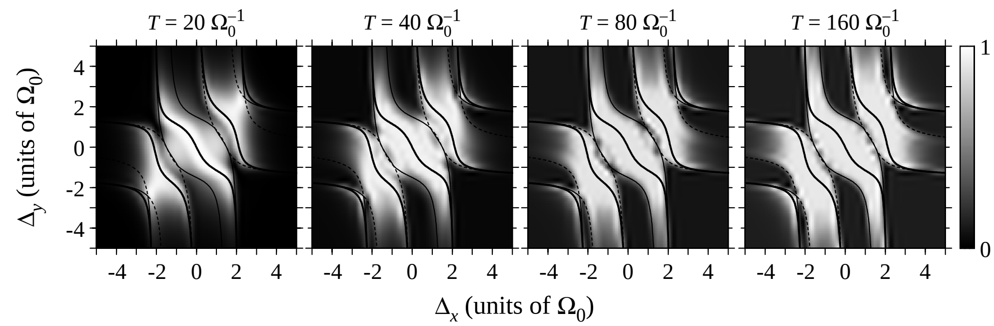

Fig. 7. The final-state population P_7 in a *seven-state system*, obtained by numerical solution of the Schrödinger equation, plotted as a function of two detunings, Δ_x and Δ_y, where $\Delta_x \equiv \Delta_2 = \Delta_3 = \Delta_4$ and $\Delta_y \equiv \Delta_5 = \Delta_6$. The curves in the ($\Delta_x$, Δ_y)-plane, on which the tuning-to-eigenvalue condition (35) is fulfilled, are shown by thick lines. The borders of the regions where the condition (38) for existence of an adiabatic-transfer state is fulfilled, are shown by thin solid or dashed curves. In all cases we have chosen the Rabi frequencies of the laser fields to be given by equations (9) and all intermediate Rabi frequencies to be equal to $\Omega_C = 3\Omega_0$. The four plots correspond to different characteristic pulse widths T.

We show the solutions to the tuning-to-eigenvalue condition (35) as thick curves. The borders of the regions in the (Δ_x, Δ_y)-plane, where the condition for existence of the AT state φ_T is fulfilled (Eq. (38)), are shown by thin solid or dashed curves. In all cases we have chosen the Rabi frequencies of the laser fields to be given by equation (9) with $f(t) = e^{-(t/T)^2}$ and $\tau = 0.5T$, and all intermediate Rabi frequencies to be equal to $\Omega_C = 3\Omega_0$. Every figure comprises four cases with different characteristic pulse widths T. For larger T the process becomes more adiabatic. The figures show that the tuning-to-eigenvalue curves lie in the middle in the AT regions. Hence, tuning to a dressed eigenstate ensures the greatest possible *robustness* of the population transfer. Put in another way, the tuning-to-eigenvalue curves are the *"backbones"* of the AT regions and the transfer efficiency there is high even when adiabaticity is not good elsewhere, as for $T = 20\Omega_0^{-1}$. The figures also show that for a certain N, there are $N-2$ AT regions and $N-2$ tuning-to-eigenvalue curves. These $N-2$ curves correspond to the $N-2$ eigenvalues of the Hamiltonian $H^{(i)}$.

4.5 Optimal dressed eigenvalues

As Figures 4, 5, 6, and 7 show, except for the case of $N = 4$, tuning to different eigenvalues leads to different results. The final-state population (the transfer efficiency) in six-state and seven-state systems is plotted in Figure 8 against the detuning Δ, where $\Delta \equiv \Delta_2 = \Delta_3 = \Delta_4 = \Delta_5$ for $N = 6$ and $\Delta \equiv \Delta_2 = \Delta_3 = \Delta_4 = \Delta_5 = \Delta_6$ for $N = 7$. The arrows indicate the values (37) at which the tuning-to-eigenvalue condition (35) is fulfilled. The Rabi frequencies of the laser fields are given by equations (9) with $f(t) = e^{-(t/T)^2}$, and all intermediate Rabi frequencies are equal to $\Omega_C = 3\Omega_0$. The characteristic pulse width is $T = 80\Omega_0^{-1}$ and the pulse delay is $\tau = 0.5T$. The upper and lower plots in Figure 8 represent essentially sections of the plots for $T = 80\Omega_0^{-1}$ in Figures 6 and 7 along lines passing throught the origin at angle $\pi/4$.

Evidently, the most favourable eigenvalues are those for which the intermediate detunings have the smallest values. This is not surprising because large detunings deteriorate adiabaticity [9]. From another point of view, the case of equal intermediate detunings means that all

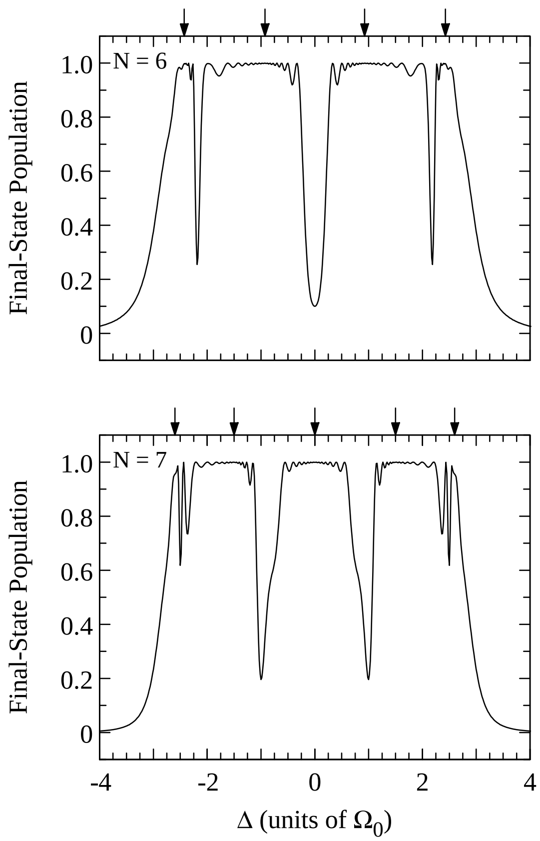

Fig. 8. The final-state populations in six-state (upper figure) and seven-state (lower figure) systems, obtained by numerical solution of the Schrödinger equation, plotted against the detuning Δ, where $\Delta \equiv \Delta_2 = \Delta_3 = \Delta_4 = \Delta_5$ for $N = 6$ and $\Delta \equiv \Delta_2 = \Delta_3 = \Delta_4 = \Delta_5 = \Delta_6$ for $N = 7$. The arrows indicate the values (37) at which the tuning-to-eigenvalue condition (35) is fulfilled. The Rabi frequencies of the laser fields are given by equations (9) with $f(t) = e^{-(t/T)^2}$, and all intermediate Rabi frequencies are equal to $\Omega_C = 3\Omega_0$. The pulse width is $T = 80\Omega_0^{-1}$ and the pulse delay is $\tau = 0.5T$.

control lasers are on exact resonance with the corresponding transitions between the bare intermediate states, while the pump and Stokes lasers are both detuned off resonance with their transitions $\psi_1 \leftrightarrow \psi_2$ and $\psi_{N-1} \leftrightarrow \psi_N$ by detunings of $-\Delta$. Larger Δ means that the pump and Stokes lasers are farther off resonance which naturally reduces the coupling of the whole system to the laser fields and the transfer efficiency.

Finally, as Figures 5 and 7 show, for odd number of states, the optimal tuning-to-eigenvalue curve is the one passing through the origin, $\Delta_x = \Delta_y = 0$. This means that for odd N, tuning all lasers on resonance with the corresponding transitions always ensures tuning to a dressed eigenvalue and moreover, to the optimal one. In contrast, as Figures 4 and 6 show, for even N, tuning to a dressed state always requires nonzero detunings [40].

5 Discussion and conclusions

We have presented a general description of how complete population transfer can be accomplished between the first and last state of a chainwise-linked system of atomic states coupled successively by pulsed lasers, with little or no transient populations in the intermediate states. The procedure generalizes the use of counterintuitive pulse sequences in the three-state STIRAP mechanism, to include arbitrary number of states. The scheme supplements the usual pump-Stokes pulse pair by one or more control pulses which connect the intermediate states. We require that the control pulses are strong and long compared with the pump and Stokes pulses, so that they are nearly constant during the times when the pump and Stokes are present. Under these conditions the original N-state system is equivalent to a system comprising $N-2$ superposed parallel Λ-transitions, in which the initial state is coupled simultaneously to $N-2$ dressed states, which in turn are coupled to the final state. These dressed states are defined as the eigenstates of the sub-Hamiltonian $H^{(i)}$, which comprises just the bare intermediate states and the couplings between them. We pointed out, with the aid of analytic expressions and numerical examples, the advantages of tuning the pump and Stokes lasers to some of these dressed states. This tuning reduces the excitation dynamics to that of an effective three-state system, eliminating the off-resonant dressed states, and it ensures maximal robustness of the population transfer against variations in the laser parameters. Moreover, this scheme applies equally well for both even and odd number of states in the chain. We have also concluded that tuning to some dressed eigenstates should be advantageous compared to others. We have found that the optimal dressed states are those, which are accessed with the smallest laser detunings in the initial, bare-state representation.

Basic tools in our analysis have been the notion of the adiabatic-transfer state, which generalizes the trapped state of the three-state STIRAP, and the notion of the intermediate dressed-state resonances, which replace the single intermediate state in STIRAP. In particular, the adiabatic-transfer state idea allows us to bound the regions in a given parameter space where adiabatic transfer can or cannot take place, as shown in Figures 4, 5, 6, and 7. The intermediate dressed resonances are simply the backbones of these AT regions and the transfer efficiency there is high even when adiabaticity is not good elsewhere. The AT state concept also tells us how far away from a dressed resonance we can go and still obtain unit efficiency for large enough T. In other words, the dressed-resonance curves show where high transfer efficiency first appears, whereas the AT regions show the borders the “white” can reach. In the non-AT (black) regions, we cannot get robust unit efficiency for any T.

The AT state concept and the analysis in this paper as a whole have been based upon the assumption of $(N-1)$-photon resonance between the initial state ψ_1 and the final state ψ_N of the chain, which corresponds to the two-photon resonance condition in the three-state STIRAP. For nonzero $(N-1)$-photon detuning, numerous avoided crossings may appear in the adiabatic picture and the explanation will be more complicated. Nevertheless, the $(N-1)$-photon resonance and the AT state idea provide a simple basis for understanding the multistate STIRAP, in the same manner as the trapped-state concept is used to explain the three-state STIRAP.

Finally, due to the similarities between the multistate scheme, presented in this work, and the three-state STIRAP, the ideas and the results in this paper can be extended in various directions in the manner in which this has been done for STIRAP. These include examining the robustness of the transfer efficiency against variations in the laser parameters (Rabi frequencies and detunings), different pulse shapes and pulse delays, verifying the insensitivity against spontaneous emission from the excited states, and others.

BWS thanks the Alexander von Humboldt Stiftung for a Research Award; his work is supported in part under the auspices of the U.S. Department of Energy at Lawrence Livermore National Laboratory under contract W-7405-Eng-48. We thank V. Malinovsky and D. Tannor for sending us a preprint of their work prior to publication. We have also benefitted from valuable discussions with Stéphane Guérin on the concept of transfer states. BWS and KB thank Vladimir Malinovsky for stimulating discussions of his work on straddle STIRAP.

Appendix: Existence of adiabatic-transfer state

We are going to show that if condition (35) is fulfilled, one of the eigenstates of H is an adiabatic-transfer state, as defined by equation (16). Let us assume that condition (35) is fulfilled. It follows from equation (29) that when $\Omega_P = 0$ and $\Omega_S = 0$ (which is by definition the case at infinity), there are *three* eigenvalues of H that vanish. Obviously, if the adiabatic-transfer state (16) exists, its eigenvalue λ_T should be one of these eigenvalues. Therefore, we have to determine the asymptotic behavior of these three eigenvalues and the corresponding eigenstates as $t \to \pm\infty$.

The early-time eigenvalues

We begin with large negative times ($t \to -\infty$). For the counterintuitive pulse sequence, Ω_P is the last pulse to appear. It follows from equation (29) that at the times when the pulse Ω_S has already arrived while the pulse Ω_P has not yet ($\Omega_P = 0$, $\Omega_S \neq 0$), only *one* eigenvalue of H vanishes. In other words, as soon as the pulse Ω_S arrives, two of the three eigenvalues, λ_1^- and λ_2^-, depart from zero while the third eigenvalue λ_0^- stays zero until the pulse Ω_P arrives (the minus signs indicate that $t \to -\infty$). At those times, $\left|\lambda_0^-\right| \ll \left|\lambda_{1,2}^-\right|$.

To determine *how* λ_0^- departs from zero when Ω_P appears, we consider the eigenvalue equation $\mathcal{D}^{(1,N)}(\lambda) \equiv \det(H/\hbar - \lambda 1) = 0$ as an implicit definition of the functional dependence of λ_0^- on Ω_P. Since in the eigenvalue equation Ω_P appears only squared, we can expand λ_0^- in terms of Ω_P^2 by using the Taylor expansion of λ_0^- *versus* Ω_P^2 with the idea to retain the lowest-order nonzero term only. We use the relation $\mathcal{D}^{(1,N)}(\lambda) = 0$ and expand $\mathcal{D}^{(1,N)}(\lambda)$ along its first and last rows to obtain

$$\lambda^2 \mathcal{D}^{(2,N-1)}(\lambda) + \frac{1}{4}\lambda \left[\Omega_P^2 \mathcal{D}^{(3,N-1)}(\lambda) + \Omega_S^2 \mathcal{D}^{(2,N-2)}(\lambda)\right] + \frac{1}{16}\Omega_P^2 \Omega_S^2 \mathcal{D}^{(3,N-2)}(\lambda) = 0, \tag{A.1}$$

where $\mathcal{D}^{(j,k)}(\lambda)$ denotes the determinant of the square matrix obtained from $(H/\hbar - \lambda 1)$ by keeping its columns from jth to kth and its rows from jth to kth as well,

$$\mathcal{D}^{(j,k)}(\lambda) = \begin{vmatrix} \Delta_j - \lambda & \frac{1}{2}\Omega_{j,j+1} & 0 & \cdots & 0 \\ \frac{1}{2}\Omega_{j,j+1} & \Delta_{j+1} - \lambda & \frac{1}{2}\Omega_{j+1,j+2} & \cdots & 0 \\ 0 & \frac{1}{2}\Omega_{j+1,j+2} & \Delta_{j+2} - \lambda & \cdots & 0 \\ \vdots & \vdots & \vdots & \ddots & \vdots \\ 0 & 0 & 0 & \cdots & \Delta_k - \lambda \end{vmatrix}. \tag{A.2}$$

None of the $\mathcal{D}$ on the right-hand side of equation (A.1) contains Ω_P or Ω_S. We differentiate equation (A.1) with respect to Ω_P^2, set $\Omega_P = 0$ and $\lambda_0^-\left(\Omega_P^2 = 0\right) = 0$, and find

$$4(d\lambda_0^-/d\Omega_P^2)_{\Omega_P^2=0}\Omega_S^2 \mathcal{D}^{(2,N-2)} + \Omega_S^2 \mathcal{D}^{(3,N-2)} = 0.$$

In order to simplify the notation, from hereafter we denote $\mathcal{D}^{(j,k)}(\lambda = 0)$ by $\mathcal{D}^{(j,k)}$. From here, we find $(d\lambda_0^-/d\Omega_P^2)_{\Omega_P^2=0}$, replace it in the Taylor expansion,

$$\lambda_0^-\left(\Omega_P^2\right) = \lambda_0^-(0) + (d\lambda_0^-/d\Omega_P^2)_{\Omega_P^2=0}\Omega_P^2 + \mathcal{O}\left(\Omega_P^4\right),$$

and keeping the lowest-order nonzero term only, we find

$$\lambda_0^- \approx -\frac{1}{4}\frac{\mathcal{D}^{(3,N-2)}}{\mathcal{D}^{(2,N-2)}}\Omega_P^2. \tag{A.3}$$

This is the desired expression for the early-time behavior of the eigenvalue which is the last to depart from zero.

In order to determine the other two eigenvalues λ_1^- and λ_2^-, which depart from zero with Ω_S, we set $\Omega_P = 0$ in equation (A.1) and divide by λ (which accounts for removing the root λ_0^-) to find

$$4\lambda \mathcal{D}^{(2,N-1)}(\lambda) + \Omega_S^2 \mathcal{D}^{(2,N-2)}(\lambda) = 0. \tag{A.4}$$

The fact that λ_1^- and λ_2^- vanish when $\Omega_S \to 0$ means that they must have expansions $\lambda_k^- = a_k \Omega_S + b_k \Omega_S^2 + \mathcal{O}(\Omega_S^3)$ $(k = 1, 2)$. Since $\mathcal{D}^{(2,N-1)}(0) = 0$ (which is the tuning condition (35)), we have $\mathcal{D}^{(2,N-1)}(\lambda) = -\mathcal{A}\lambda + \mathcal{O}(\lambda^2)$. The constant $\mathcal{A}$ can easily be found from equation (29); it is

$$\mathcal{A} = \sum_{k=2}^{N-1} \mathcal{D}^{(2,k-1)}\mathcal{D}^{(k+1,N-1)}, \tag{A.5}$$

where, as above, $\mathcal{D}^{(j,k)} \equiv \mathcal{D}^{(j,k)}(\lambda = 0)$, and the convention $\mathcal{D}^{(n,n+1)} = 1$ is used. In order to find the asymptotic behaviors of λ_1^- and λ_2^-, we need to keep only the lowest order terms with respect to Ω_S in equation (A.4). Hence, we substitute $\mathcal{D}^{(2,N-1)}(\lambda) = -\mathcal{A}\lambda + \mathcal{O}(\lambda^2)$ and $\mathcal{D}^{(2,N-2)}(\lambda) = \mathcal{D}^{(2,N-2)} + \mathcal{O}(\lambda)$ and find

$$-4\mathcal{A}\lambda^2 + \Omega_S^2 \mathcal{D}^{(2,N-2)} = 0. \tag{A.6}$$

The two real solutions of this equation, if they exist, give the asymptotic behaviors of λ_1^- and λ_2^- for small Ω_S,

$$\lambda_1^- \approx -\frac{\Omega_S}{2}\sqrt{\frac{\mathcal{D}^{(2,N-2)}}{\mathcal{A}}}, \quad \lambda_2^- \approx \frac{\Omega_S}{2}\sqrt{\frac{\mathcal{D}^{(2,N-2)}}{\mathcal{A}}}\cdot \tag{A.7}$$

These solutions will be real if $\mathcal{D}^{(2,N-2)}$ and $\mathcal{A}$ have the same sign. In order to verify this we use the relation

$$\mathcal{D}^{(2,k)}\mathcal{D}^{(k+1,N-1)} = \frac{1}{4}\Omega_{k,k+1}^2 \mathcal{D}^{(2,k-1)}\mathcal{D}^{(k+2,N-1)}, \quad (k = 2, 3, \ldots, N-2), \tag{A.8}$$

which follows from $\mathcal{D}^{(2,N-1)} = 0$ and can easily be proved by induction. By rewriting it in the form

$$\frac{\mathcal{D}^{(2,k)}}{\mathcal{D}^{(k+2,N-1)}} = \frac{1}{4}\Omega_{k,k+1}^2 \frac{\mathcal{D}^{(2,k-1)}}{\mathcal{D}^{(k+1,N-1)}}, \tag{A.9}$$

we conclude that in the sum (A.5), the term $\mathcal{D}^{(2,k-1)}\mathcal{D}^{(k+1,N-1)}$ has the same sign as the next term $\mathcal{D}^{(2,k)}\mathcal{D}^{(k+2,N-1)}$ for any k. Hence, all terms in the sum have the same sign. Since the last term (for $k = N-1$) is $\mathcal{D}^{(2,N-2)}$, it follows that $\mathcal{A}$ has the same sign as $\mathcal{D}^{(2,N-2)}$ and thus, the two roots (A.7) of equation (A.6), are real.

The late-time eigenvalues

In a similar manner, we find that for $t \to +\infty$, the three vanishing eigenvalues behave as

$$\lambda_0^+ \approx -\frac{1}{4}\frac{\mathcal{D}^{(3,N-2)}}{\mathcal{D}^{(3,N-1)}}\Omega_S^2, \tag{A.10}$$

$$\lambda_1^+ \approx -\frac{\Omega_P}{2}\sqrt{\frac{\mathcal{D}^{(3,N-1)}}{\mathcal{A}}}, \quad \lambda_2^+ \approx \frac{\Omega_P}{2}\sqrt{\frac{\mathcal{D}^{(3,N-1)}}{\mathcal{A}}}. \tag{A.11}$$

In the derivation of equations (A.3, A.7, A.10, A.11),it has been assumed that $\mathcal{D}^{(2,N-2)} \neq 0$ and $\mathcal{D}^{(3,N-1)} \neq 0$. It is easily seen that this is the case by using the relation

$$\mathcal{D}^{(2,k-1)}\mathcal{D}^{(3,k)} = \mathcal{D}^{(2,k)}\mathcal{D}^{(3,k-1)} + \frac{1}{2^{2k-4}}\Omega_{2,3}^2\Omega_{3,4}^2 \ldots \Omega_{k-1,k}^2, \tag{A.12}$$

which can readily by proved by induction. By setting $k = N-1$ in it, we find that if $\mathcal{D}^{(2,N-1)} = 0$, then

$$\mathcal{D}^{(2,N-2)}\mathcal{D}^{(3,N-1)} = \frac{1}{2^{2N-6}}\Omega_{2,3}^2\Omega_{3,4}^2 \ldots \Omega_{N-2,N-1}^2 > 0. \tag{A.13}$$

Connectivity

It is straightforward to show that the eigenstate associated with λ_0^- tends to state ψ_1 as $t \to -\infty$ and the eigenstate associated with λ_0^+ tends to state ψ_N as $t \to +\infty$. Hence, if λ_0^- and λ_0^+ correspond to *the same* eigenvalue, the corresponding eigenstate will be the desired AT state φ_T, equation (16). In the general case of arbitrary laser parameters, this may or may not happen [40]. However, in the present case, when the lasers are tuned to an eigenvalue of $H^{(i)}$ and hence, the asymptotic behaviors of the three vanishing eigenvalues are given by equations (A.3, A.7, A.10, A.11), the eigenvalue λ_0^- always connects to λ_0^+ and we are guaranteed that the AT state exists.

To show this we first note that the eigenvalues, which do *not* vanish as $t \to \pm\infty$, *do not interfere* in the linkages between the vanishing eigenvalues because each of the nonvanishing eigenvalues $\lambda_n(t)$ tends to $\lambda_n(-\infty) \neq 0$ as $t \to -\infty$ and to $\lambda_n(+\infty) \neq 0$ as $t \to +\infty$. Moreover, since the Hamiltonian (29) has the same form when $t \to \pm\infty$, we have $\lambda_n(+\infty) = \lambda_n(-\infty)$. Hence, the eigenvalues that are above (below) the three vanishing eigenvalues at $-\infty$ remain above (below) them at $+\infty$ as well, because the eigenvalues cannot cross.

Let us now consider the connections between the three vanishing eigenvalues. Insofar as $\Omega_P/\Omega_S \to 0$ as $t \to -\infty$, we have $\lambda_1^- < \lambda_0^- < \lambda_2^-$. Also, since $\Omega_S/\Omega_P \to 0$ as $t \to +\infty$, we have $\lambda_1^+ < \lambda_0^+ < \lambda_2^+$. This means that the connections $\lambda_1^- \leftrightarrow \lambda_1^+$, $\lambda_0^- \leftrightarrow \lambda_0^+$, and $\lambda_2^- \leftrightarrow \lambda_2^+$ take place, and therefore, the adiabatic-transfer state φ_T always exists when the lasers are tuned to an eigenstate of the subsystem Hamiltonian $H^{(i)}$.

References

1. B.W. Shore, *The Theory of Coherent Atomic Excitation* (Wiley, New York, 1990).
2. J. Oreg, F.T. Hioe, J.H. Eberly, Phys. Rev. A **29**, 690 (1984).
3. J.R. Kuklinski, U. Gaubatz, F.T. Hioe, K. Bergmann, Phys. Rev. A **40**, 6741-44 (1989).
4. B.W. Shore, K. Bergmann, J. Oreg, Z. Phys. D **23**, 33 (1992).
5. B.W. Shore, K. Bergmann, A. Kuhn, S. Schiemann, J. Oreg, J.H. Eberly, Phys. Rev. A **45**, 5297 (1992).
6. K. Bergmann, B.W. Shore, in *Molecular Dynamics and Spectroscopy by Stimulated Emission Pumping*, edited by H.L. Dai, R.W. Field (World Scientific, Singapore, 1995).
7. B.W. Shore, Contemp. Phys. **36**, 15-28 (1995).
8. K. Bergmann, H. Theuer, B.W. Shore, Rev. Mod. Phys. **70**, 1003 (1998).
9. N.V. Vitanov, S. Stenholm, Opt. Commun. **135**, 394 (1997).
10. N.V. Vitanov, S. Stenholm, Phys. Rev. A **56**, 1463 (1997).
11. U. Gaubatz, P. Rudecki, M. Becker, S. Schiemann, M. Külz, K. Bergmann, Chem. Phys. Lett. **149**, 463 (1988).
12. U. Gaubatz, P. Rudecki, S. Schiemann, K. Bergmann, J. Chem. Phys. **92**, 5363 (1990).
13. H.-G. Rubahn, E. Konz, S. Schiemann, K. Bergmann, Z. Phys. D **22**, 401 (1991).

14. A. Kuhn, S. Schiemann, G.Z. He, G. Coulston, W.S. Warren, K. Bergmann, J. Chem. Phys. **96**, 4215 (1992).
15. P. Dittmann, F.P. Pesl, J. Martin, G.W. Coulston, G.Z. He, K. Bergmann, J. Chem. Phys. **97**, 9472 (1992).
16. S. Schiemann, A. Kuhn, S. Steuerwald, K. Bergmann, Phys. Rev. Lett. **71**, 3637 (1993).
17. J. Lawall, M. Prentiss, Phys. Rev. Lett. **72**, 993 (1994).
18. T. Halfmann, K. Bergmann, J. Chem. Phys. **104**, 7078 (1996).
19. A. Kuhn, S. Steuerwald, K. Bergmann, Eur. Phys. J. D **1**, 57 (1998).
20. G. Coulston, K. Bergmann, J. Chem. Phys. **96**, 3467 (1992).
21. Y.B. Band, P.S. Julienne, J. Chem. Phys. **94**, 5291 (1991).
22. Y.B. Band, P.S. Julienne, J. Chem. Phys. **96**, 3339 (1992).
23. B.W. Shore, J. Martin, M.P. Fewell, K. Bergmann, Phys. Rev. A **52**, 566 (1995).
24. J. Martin, B.W. Shore, K. Bergmann, Phys. Rev. A **52**, 583 (1995).
25. J. Martin, B.W. Shore, K. Bergmann, Phys. Rev. A **54**, 1556 (1996).
26. M.V. Danileiko, V.I. Romanenko, L.P. Yatsenko, Opt. Commun. **109**, 462 (1994).
27. V.I. Romanenko, L.P. Yatsenko, Opt. Commun. **140**, 231 (1997).
28. M.P. Fewell, B.W. Shore, K. Bergmann, Austral. J. Phys. **50**, 281 (1997).
29. B.W. Shore, K. Bergmann, J. Oreg, S. Rosenwaks, Phys. Rev. A **44**, 7442 (1991).
30. P. Marte, P. Zoller, J.L. Hall, Phys. Rev. A **44**, R4118 (1991).
31. A.V. Smith, J. Opt. Soc. Am. B **9**, 1543 (1992).
32. J. Oreg, K. Bergmann, B.W. Shore, S. Rosenwaks, Phys. Rev. A **45**, 4888 (1992).
33. V.S. Malinovsky, D.J. Tannor, Phys. Rev. A **56**, 4929 (1997).
34. P. Pillet, C. Valentin, R.-L. Yuan, J. Yu, Phys. Rev. A **48**, 845 (1993).
35. C. Valentin, J. Yu, P. Pillet, J. Phys. II France **4**, 1925 (1994).
36. L. Goldner, C. Gerz, R. Spreeuw, S. Rolston, C. Westbrook, W. Phillips, P. Marte, P. Zoller, Phys. Rev. Lett. **72**, 997 (1994).
37. H. Theuer, K. Bergmann, Eur. Phys. J. D **2**, 279 (1998).
38. B.W. Shore, R.J. Cook, Phys. Rev. A **20**, 1958 (1979).
39. B.W. Shore, Phys. Rev. A **24**, 1413 (1981).
40. N.V. Vitanov, Phys. Rev. A **58**, 2295 (1998).
41. S. Chelkowski, A.D. Bandrauk, P.B. Corkum, Phys. Rev. Lett. **65**, 2355 (1990).
42. J.S. Melinger, S.R. Gandhi, A. Hariharan, D. Goswami, W.S. Warren, J. Chem. Phys. **101**, 6439 (1994).
43. S. Chelkowski, A.D. Bandrauk, J. Raman Spectrosc. **28**, 459 (1997).
44. S. Guerin, Phys. Rev. A **56**, 1458 (1997).